Appl Phys B (2012) 107:137–143
DOI 10.1007/s00340-011-4862-z

Applied Physics B
Lasers and Optics

Ultrafast heat transfer on nanoscale in thin gold films

K.V. Poletkin · G.G. Gurzadyan · J. Shang · V. Kulish

Received: 26 July 2011 / Revised version: 30 October 2011 / Published online: 14 January 2012

Abstract Heat transfer processes, induced by ultrashort laser pulses in thin gold films, were studied with a time resolution of 50 fs. It is demonstrated that in thin gold films heat is transmitted by means of electron–phonon and phonon–phonon interactions, and dissipated on nanoscale within 800 fs. Measurements show that the electron–phonon relaxation time varies versus the probe wavelength from 1.6 to 0.8 ps for $\lambda = 560$–630 nm. The applied mathematical model is a result of transforming the two-temperature model to the hyperbolic heat equation, based on assumptions that the electron gas is heated up instantaneously and applying Cattaneo's law to the phonon subsystem, agrees well with the experimental results. This model allows us to define time of electron–phonon scattering as the ratio of the heat penetration depth to the speed of sound in the bulk material that, in turn, provides an explanation of experimental results that show the dependence of the electron–phonon relaxation time on the wavelength.

1 Introduction

Understanding heat transfer processes in metallic films induced by ultrashort laser pulse is of great importance due to their wide applications in microelectronics [1], micro- and nano-electro mechanical devices, data storage devices [2, 3], etc.

In order to theoretically and numerically study the laser interaction with metallic films, the two-temperature model (TTM) proposed by Anisimov [4] is widely employed [5]. In general, the TTM is written in the form of two coupled nonlinear parabolic partial differential equations that describe interaction of two subsystems, the electron and phonon (lattice) gasses. The model is based on the assumption that electrons and phonons are in thermal equilibrium. In particular, that was in detail considered by Tzou [6], who then proposed a macroscopic dual-phase-lag theory. This theory is a result of modification of the TTM to one partial differential equation that reflects the effect of microscopic phonon–electron interaction and diffusion.

Numerous experimental studies of metallic films heating by laser with picosecond and subpicosecond pulses have been performed [7–14] and show that a finite time is needed to reach the electron–phonon thermal equilibrium. It means that irradiation by an ultrashort laser pulse can transiently bring the metallic film to a stage of strong electron–phonon nonequilibrium, in which the electron gas temperature rises whereas the phonon (lattice) gas remains unchanged. The strong electron–phonon nonequilibrium stage in metallic films is a totally different thermal response of the metallic film compared to a prediction from the original TTM but can still be included within the framework of TTM. To reflect this nonequilibrium stage in films, Qiu and Tien [15] rigorously derived a hyperbolic two-step model from the Boltzmann transport equation for electrons. Klossika et al. [16] extended the TTM by Cattaneo's law for the heat flux in the electron gas to account for a finite propagation speed of heat. Also, Chen and Beraun [17] applied Cattaneo's law for both electron and phonon subsystems

K.V. Poletkin · V. Kulish (✉)
Division of Thermal and Fluids Engineering, School of Mechanical & Aerospace Engineering, Nanyang Technological University, 50 Nanyang Ave., Singapore 639798, Singapore
e-mail: MVVKulish@ntu.edu.sg

G.G. Gurzadyan (✉) · J. Shang
Division of Physics and Applied Physics, School of Physical & Mathematical Sciences, Nanyang Technological University, 21 Nanyang Link, Singapore 637371, Singapore
e-mail: gurzadyan@ntu.edu.sg

and performed numerical analysis of the proposed model, which, in general, is a set of four partial differential equations.

Due to physical complexity of the ultrafast heat transfer mechanism in metallic films, the proposed models, as a rule, do not have analytical solutions and are analyzed numerically. This fact requires further investigations of developed models theoretically as well as experimentally, to clarify the physical essence of ultrafast heat transfer mechanism in metallic films.

In this article, the results of experimental and theoretical studies of heat transfer processes in thin gold films induced by 100-fs laser pulses with a time resolution of 50 fs are presented. The analysis of experimental results shows that the heat transfer in thin gold films occurs via electron–phonon and phonon–phonon interactions and that the resulting temperature wave is dissipated in a surface layer of thin film within 800 fs. Observed decay times of 1.6 to 0.8 ps correspond to the electron–phonon relaxation, and 12 ps corresponds to the phonon–phonon relaxation. Moreover, the electron–phonon relaxation time varies versus the probe wavelength; at the same time, the phonon–phonon relaxation time shows a weak dependence on the probe wavelength.

Due to a small heat capacity of the electron gas, thermalization caused by electron–electron interactions [18, 19] takes place during a time scale less than few hundred femtoseconds. This time is relatively small referring to the total duration of the surface temperature response, which takes more than 10 ps. Thus, the heating of the electron gas is assumed to be instantaneous, and, applying Cattaneo's law to the phonon subsystem of TTM allows one to transform the model into the hyperbolic heat equation [20]. The developed model taking into account the both sources, i.e., the volumetric and surface heat flux, is studied analytically within a semi-infinite domain and agrees well with the experimental data. This model allows us to define the time of electron–phonon relaxation as the ratio of the penetration depth to the speed of sound in the bulk material. Since the dependence of the penetration depth on the wavelength has been experimentally observed, for instance, in [21], the definition of the electron–phonon relaxation time has a physical meaning and provides an explanation of experimental results which show dependence of the electron–phonon relaxation time on the wavelength.

2 Experimental setup

The pump-probe transient reflection experimental setup is shown in Fig. 1. The output of Titanium–Sapphire (Legend Eite, Coherent) regenerative amplifier seeded by an oscillator (Micra, Coherent) was used as a pulse laser source: wavelength 800 nm, pulse width 65 fs, pulse repetition rate 1 kHz, average power 3.5 W. The main part, 90%, of the radiation was converted into the UV (350 nm) by the use of the optical parametric oscillator (Topas, Light Conversion) with the following second- and fourth-harmonic generation and was used as pump pulse. The remaining 10% was used to generate white light continuum in a CaF_2 plate, i.e., the probe pulse [22].

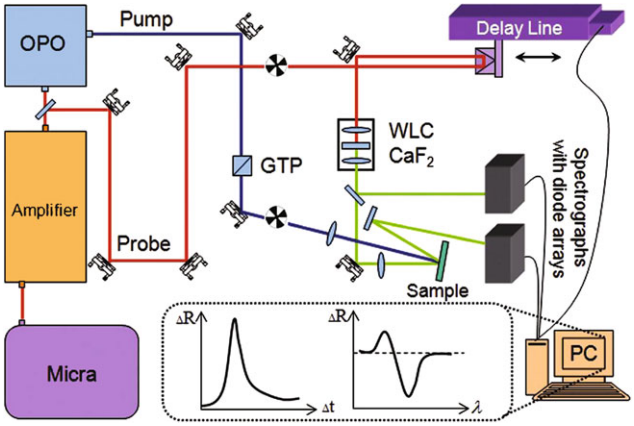

Fig. 1 Pump-probe transient reflection: OPO is the Optical Parametric Oscillator; GTP is the Glan–Thompson Polarizer; WLC is the White Light Continuum

Pump pulses (fluence ~40 μJ/cm^2) were focused on the surface of a 300-μm-thick gold film deposited on a SiO_2 substrate with a lens of 30-cm focal length and an incidence angle of 10°. Probe pulses with variable time delays relative to pump pulses were used to measure time-resolved transient reflection produced by the pump pulses. The white light continuum was split into two beams (probe and reference) and, after reflection from the sample, directed into two diode arrays attached to spectrometers (Model 77400, Oriel). According to [6, 23], at early times after 100-fs laser excitation, the normalized reflectivity change $\Delta R/R$ is proportional to the normalized temperature change of the electron gas $\Delta T/T$:

$$\frac{\Delta T}{T} \sim \frac{\Delta R}{R}. \tag{1}$$

Thus, the surface reflectivity kinetics were obtained and assigned to the surface temperature variations.

3 Experimental results

Figures 2, 3, and 4 show normalized reflection changes at 561, 590, and 632 nm, respectively, after 350-nm excitation of the gold films deposited on a quartz substrate (open circles: experimental data; solid curves: applied theocratical model, see below).

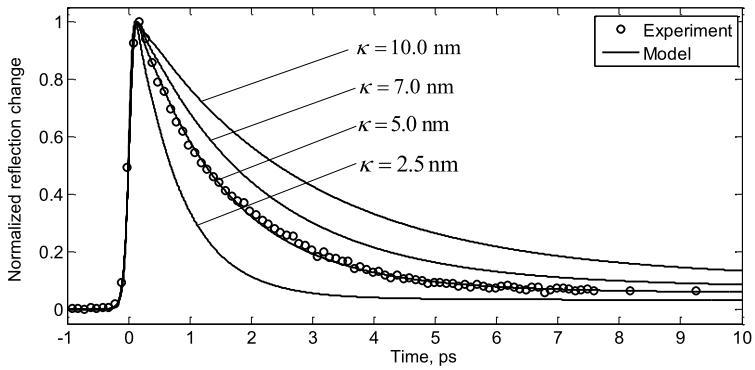

Fig. 2 Decay kinetics of the reflection change at 561 nm from 300 μm gold plated quartz substrate after the excitation with 350-nm 65-fs laser pulse and theoretical curves for different penetration depths κ

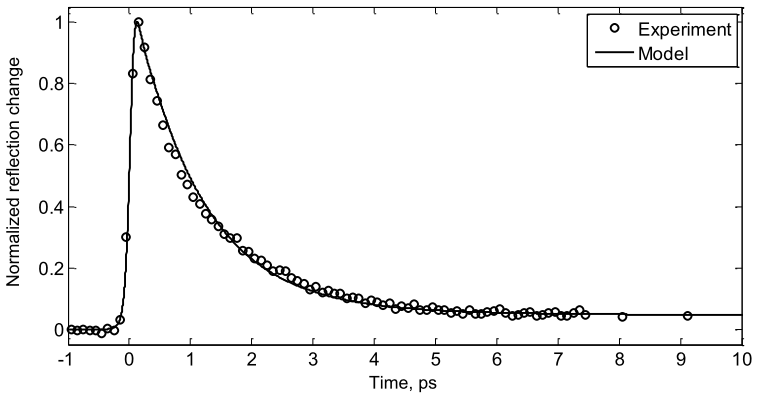

Fig. 3 Decay kinetics of the reflection change at 590 nm from 300 μm gold plated quartz substrate after the excitation with 350-nm 65-fs laser pulse and theoretical curves for penetration depth $\kappa = 3.8$ nm corresponding to electron–phonon relaxation time equal to 1.15 ps

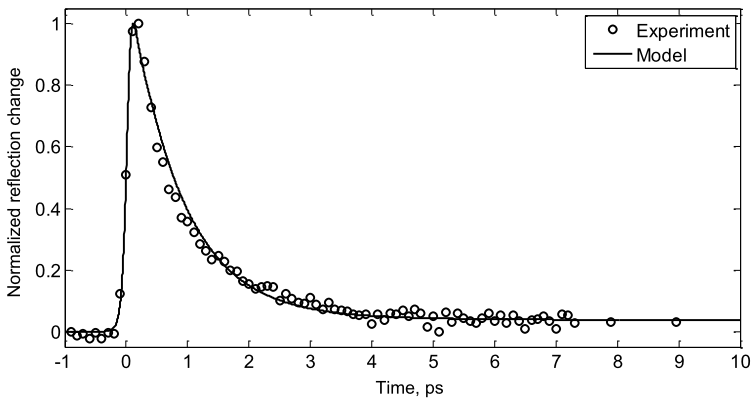

Fig. 4 Decay kinetics of the reflection change at 632 nm from 300 μm gold plated quartz substrate after the excitation with 350-nm 65-fs laser pulse and theoretical curves for penetration depth $\kappa = 3.0$ nm corresponding to electron–phonon relaxation time equal to 0.9 ps

The experimental data in the time range $t = 0$–5 ps were also fitted to a multiexponential decay function convoluted with the instrument response function $B(t - t_0)$ centered at t_0:

$$\Delta R(t) = \int_0^\infty \left(\sum_{i=1}^{n} \Delta R_i \exp\left(-\frac{t'}{\tau_i}\right) \right) \times B\left(t - t' - t_0\right) dt', \quad (2)$$

where $\Delta R(t)$ is the differential reflection at time t, ΔR_i is the amplitude of component with lifetime τ_i. The full-width-half-maximum (FWHM) of the instrument response function, taken from the pump-probe cross-correlation signal in quartz, was 100 ± 10 fs.

Table 1 Deconvolution-fit results of rise and decay times of the reflection change in gold films after 350-nm excitation

Probe wavelength, [nm]	561	590	632
Rise time, [fs]	<100	<100	<100
Decay time, [ps]	1.63	1.27	0.87

Table 1 shows fit results. Rise times at all probe wavelengths were less than 100 fs. Decay times decrease from 1.63 to 0.87 ps by changing the probe wavelengths from 561 to 632 nm.

4 Mathematical model

In general, the TTM can be expressed in terms of two coupled nonlinear partial differential equations for one-dimensional problem as follows:

$$C_e(T_e)\frac{\partial T_e}{\partial t} = \frac{\partial}{\partial x}\left[k_e(T_e, T_p)\frac{\partial T_e}{\partial x}\right] - G(T_e)(T_e - T_p) + S(x,t), \quad (3)$$

$$C_p(T_p)\frac{\partial T_p}{\partial t} = \frac{\partial}{\partial x}\left[k_p(T_p)\frac{\partial T_p}{\partial x}\right] + G(T_e)(T_e - T_p), \quad (4)$$

where C and k are the heat capacities and thermal conductivities of the electrons and phonons as denoted by subscripts e and p, respectively, $G(T_e)$ is the electron–phonon coupling factor, and $S(x,t)$ is a source term describing the local energy deposition by the laser pulse. The model is based on the assumption that electrons and phonons are in thermal equilibrium. Observations of experimental data show that the thermalization of the electron gas due to electron–electron interactions takes place during a time scale less than few hundred femtoseconds [18, 19]. This time is relatively small in comparison with the total duration of the surface temperature response, which takes more than 10 ps. Thus, the heating of the electron gas is assumed to be instantaneous, so in (3) the terms $C_e(T_e)\frac{\partial T_e}{\partial t}$ and $\frac{\partial}{\partial x}[k_e(T_e, T_p)\frac{\partial T_e}{\partial x}]$ do not have effect on the process of heating the electron gas. Hence, (3) can be simplified and becomes

$$G(T_e)(T_e - T_p) \approx S(x,t). \quad (5)$$

Equation (5) shows that equilibrium between electron and phonon gases occurs after the laser excitation.

Although material parameters C_p, k_p, and G are, in general, functions of temperature, in our study we treat them as constants. As the relaxation time of the phonon gas in metal is about 10 ps, we extend (4) by applying Cattaneo's law for the heat flux in the phonon gas, which is

$$\tau\frac{\partial q_p''}{\partial t} + q_p'' = -k_p\frac{\partial T_p}{\partial x}, \quad (6)$$

where τ is the relaxation time, and q_p'' is the heat flux of the phonon gas corresponding to the gradient of T_p. Combining (6) with (4) and accounting for the law of energy conservation, we have

$$\tau\frac{\partial^2 T_p}{\partial t^2} + \frac{\partial T_p}{\partial t} = \alpha_p\frac{\partial^2 T_p}{\partial x^2} + \frac{1}{C_p}\left[G(T_e - T_p) + \tau\frac{\partial}{\partial t}G(T_e - T_p)\right], \quad (7)$$

where $\alpha_p = k_p/C_p$ is the thermal diffusivity of the phonon gas. Substituting (5) into (7), a one-dimensional hyperbolic heat equation [20] with the time-dependent volumetric heat source is obtained and can be written as follows:

$$\tau\frac{\partial^2 T}{\partial t^2} + \frac{\partial T}{\partial t} = \alpha\frac{\partial^2 T}{\partial x^2} + \left[q + \tau\frac{\partial q}{\partial t}\right], \quad (8)$$

where $q = S(x,t)/C$ ($C \equiv C_p$, see below). Due to the assumption mentioned above that the electron gas is heated instantaneously, electron–phonon subsystems are at equilibrium. Hence, all parameters of (8) can be defined as for the bulk material, and the subscript p is removed from the equation.

Note that Klossika studied the propagation of heat in a metal by means of waves with a finite speed, however, in his considerations the volumetric heat source was neglected [16]. In our case, the penetration depth is of the order of few nanometers. Nevertheless, the basic term which defines the surface temperature response under our experimental conditions (subpicosecond irradiation) is not the surface heat flux, but the volumetric source. Moreover, the penetration depth, which is included in the volumetric source, is an important characteristic that defines the relaxation time of electron–phonon scattering in metal thin films. Hence, the volumetric source cannot be neglected in a realistic model.

For the further analysis, (8) is rewritten in a dimensionless form

$$\frac{\partial^2\theta}{\partial\xi^2} + 2\frac{\partial\theta}{\partial\xi} = \frac{\partial^2\theta}{\partial\eta^2} + \left[\tilde{q} + \frac{1}{2}\frac{\partial\tilde{q}}{\partial\xi}\right], \quad (9)$$

where $\xi = t/(2\tau)$, $\eta = x/(2\sqrt{\alpha\tau})$, and θ and $\tilde{q}$ are the dimensionless temperature and volumetric sources, respectively.

It is assumed that the light intensity of the laser pulse, denoted by $I(t)$, is Gaussian and the laser irradiation energy is absorbed by the metallic film exponentially. Upon correcting the reflection at the surface, the volumetric heating within the material can be simulated as

$$S(x,t) = \frac{1-R}{\kappa}\exp\left(-\frac{x}{\kappa}\right)I(t), \quad (10)$$

where R is the reflectivity of the irradiated surface, and κ is the radiation penetration depth. The dimensionless temperature can be defined as

$$\theta = \frac{C\rho\sqrt{\alpha\tau\pi}}{F(1-R)}[T - T_0], \quad (11)$$

where F is the fluence of the laser radiation, and T_0 is the initial temperature; hence, the dimensionless volumetric source becomes

$$\tilde{q} = \frac{1}{\xi_p\Delta\eta}\exp\left(-\frac{\eta}{\Delta\eta} - a\left[\frac{\xi - \xi_b}{\xi_p}\right]^2\right), \quad (12)$$

where $\xi_p = t_p/(2\tau)$, $\xi_b = t_b/(2\tau)$, $\Delta\eta = \kappa/(2\sqrt{\alpha\tau})$, a is a positive constant (e.g., for the Gaussian distribution, $a = 2.77$ [15]), and t_p is the FWHM of the laser pulse.

Now, we are going to obtain the solution to (9) by the use of the method proposed in [24], which was further developed for finite domains [25] and for nonhomogeneous problems [26]. This method leads to a Volterra-type integral equation that relates the local values of temperature and the corresponding heat flux. The equation is valid in the entire domain, including the boundaries.

Details of the solution procedure of (9) in the Laplace space are shown in the Appendix. According to this procedure, the general solution in its complete form is

$$Q(\eta;s)=\frac{1+\frac{1}{2}s}{\lambda(s)}\tilde{Q}''(s)+P(\eta;s)+\frac{1}{\lambda(s)}\frac{dP(\eta;s)}{d\eta}, \quad (13)$$

where

$$P(\eta;s)=\Delta\eta^2\frac{1+\frac{1}{2}s}{\Delta\eta^2s^2+2\Delta\eta^2s-1}\tilde{Q}(\eta;s). \quad (14)$$

Analysis of (14) shows that the latter defines two processes which are due to electron–phonon and phonon–phonon scattering, characterized by the denominator of the transfer function and numerator, respectively. It is known that relaxation time τ is defined as

$$\tau=\frac{\alpha}{c^2}, \quad (15)$$

where c is a speed of sound in a bulk material and corresponds to phonon–phonon scattering [27]. Hence, taking into account the definition for τ (15) and dimensionless constant $\Delta\eta$, the relaxation time corresponding to electron–phonon scattering can be defined as follows:

$$\tau_{e-\mathrm{ph}}=\frac{\kappa}{c}. \quad (16)$$

By substituting (14) into (13) and finding the inverse Laplace transform, the solution of (9) can be presented in the integral form. For the surface temperature ($\eta=0$), it becomes

$$\begin{aligned}\theta(\xi)=&\int_0^{\xi}\left[\tilde{q}''(\xi^*)+\frac{1}{2}\frac{\partial\tilde{q}''(\xi^*)}{\partial\xi^*}\right]I_0(\xi-\xi^*)e^{-(\xi-\xi^*)}\,d\xi^*\\&+\frac{\Delta\eta^2}{4\sqrt{1+\Delta\eta^2}}\sqrt{\frac{\pi}{a}}\int_0^{\xi}\left\{\left(1+\frac{1}{2}s_1\right)e^{\frac{B_1^2}{A}}\right.\\&\times\left[\mathrm{erf}\left(\sqrt{A}\xi^*+\frac{B_1}{\sqrt{A}}\right)-\mathrm{erf}\left(\frac{B_1}{\sqrt{A}}\right)\right]\\&-\left(1+\frac{1}{2}s_2\right)e^{\frac{B_2^2}{A}}\left[\mathrm{erf}\left(\sqrt{A}\xi^*+\frac{B_2}{\sqrt{A}}\right)\right.\\&\left.\left.-\mathrm{erf}\left(\frac{B_2}{\sqrt{A}}\right)\right]\right\}\left(\delta(\xi-\xi^*)\right.\\&\left.-\frac{1}{\Delta\eta}I_0(\xi-\xi^*)e^{-(\xi-\xi^*)}\right)d\xi^*, \quad (17)\end{aligned}$$

where $I_0(\xi)$ is the modified Bessel function, $\delta(\xi)$ is the Dirac delta function, $\mathrm{erf}(\xi)$ is the Gauss error function [28], $s_{1,2}=-1\pm\frac{1}{\Delta\eta}\sqrt{1+\Delta\eta^2}$, $B_{1,2}=s_{1,2}-2\frac{a}{\xi_p^2}\xi_b$, and $A=\frac{a}{\xi_p^2}$.

Thus a model, based on the assumption that the heating of the electron gas is instantaneous, has been developed (see (17)). It shows that the heat transfer in thin metallic films occurs initially by means of electron–phonon interaction, followed by phonon–phonon interaction. The model predicts that the electron–phonon thermal equilibrium occurs after the laser excitation and defines the electron–phonon relaxation time as the ratio of the penetration depth to the speed of sound in the bulk material, see (16). The model describes the surface temperature response of the thin film induced by an ultrashort laser pulse and takes into account contributions of the transient heat flux (given by the first integral in (17)) and the volumetric heat source (the second integral in (17)).

5 Model analysis and validation

The first and second integrals in (17) are denoted by $\theta_f(\xi)$ and $\theta_v(\xi)$, respectively. Contributions of $\theta_f(\xi)$ and $\theta_v(\xi)$ are different and depend on ξ_p and $\Delta\eta$. Note that, in a particular case, the dependence of the local temperature on $\theta_f(\xi)$ has been studied in [29]. However, the analysis of model (17) shows that for $\xi_p<0.02$ and $0.01<\Delta\eta<0.15$ (chosen from practical reasons to fulfill conditions of the performed experiment), the contribution of the surface heat flux $\theta_f(\xi)$ becomes negligible in comparison with the contribution of $\theta_v(\xi)$. Hence, model (17) can be simplified as

$$\theta(\xi)\approx\theta_v(\xi). \quad (18)$$

The surface temperature is monitored up to 400 ps, after the laser excitation. For direct comparison of the model with experimental data, we use the normalized temperature. A maximal temperature change, estimated from (11), is 350 K. Hence, we are operating in the linear range of reflectivity versus the temperature [30, 31]. Gold properties and their dependence on temperature are presented in Table 2. The variation of the relaxation time τ is only 2.7% in the temperature range between 300 and 500 K. Thus, the influence of the local surface temperature variations on τ is negligible, and the relaxation time can be taken as 12 ps.

Hence, taking into account the value of the relaxation time and the time characteristics of the laser pulse, the dimensionless variable $\xi_p=4.2\times10^{-3}$. Since heat is dissipated in a surface layer of the gold film and the radiation penetration depth lies within the range between 2 and 10 nm or, in the dimensionless form, between 0.03 and 0.1, (18) can be used to perform numerical simulations.

Figure 2 shows comparison of the experimental results at the probe wavelength 561 nm with the developed model under variations of the radiation penetration depth. We found a good agreement between theoretical model (18) and experimental results for the penetration depth of 5.0 nm that

Table 2 Temperature-dependent bulk properties of gold

Temperature, [K]	300	400	500
Thermal diffusivity[a] α, [m^2/s]	1.27×10^{-4}	1.22×10^{-4}	1.19×10^{-4}
Speed of sound[b] c, [m/s]	3280	3200	3140
Relaxation time[c] τ, [ps]	12	12	12

[a]Reference [32]

[b]Reference [33]

[c]Calculated by (15)

corresponds to electron–phonon relaxation time calculated by (16) $\tau_{e-\mathrm{ph}} = 1.52$ ps and phonon–phonon relaxation time $\tau = 12$ ps.

Figures 3 and 4 present experimentally measured kinetics of the reflection changes at 590 and 632 nm, respectively, together with the theoretically obtained data. Calculations were performed for the radiation penetration depths of 3.8 and 3.0 nm which correspond to electron–phonon relaxation times calculated by (16) $\tau_{e-\mathrm{ph}} = 1.15$ and 0.9 ps, respectively.

6 Conclusion

Heat transfer processes in thin gold films induced by 100-fs laser pulses are studied both experimentally and theoretically. The analysis of experimental results shows that the heat transfer in thin gold films occurs via electron–phonon and phonon–phonon interactions and the resulting temperature wave is dissipated in a surface layer of thin films within 800 fs. Electron–phonon relaxation time varies in the range from 1.6 to 0.8 ps with the wavelength $\lambda = 560$–630 nm. The phonon–phonon relaxation time is equal to 12 ps and shows a weak dependence on the probe wavelength.

The proposed model is a result of transformation of TTM to the hyperbolic heat equation based on the assumptions that the electron gas is heated instantaneously and Cattaneo's law is applied to the phonon subsystem. This model is studied analytically within a semi-infinite domain with both the volumetric and the surface heat flux energy sources and agrees well with the experimental data. The view of heat processes proposed here allows us to define the time of electron–phonon relaxation as a ratio of the penetration depth to the speed of sound in the bulk material. In turn, this definition of the electron–phonon relaxation time provides an explanation of experimental results which show the dependence of the electron–phonon relaxation time on the wavelength and agrees well with the experiment.

Acknowledgements The authors are thankful to Prof. M.E. Michel-Beyerle for continuous support. This work is supported by the Singapore Agency for Science, Technology and Research (A*STAR), under research grant SERC GRANT No. 092 156 0123.

Appendix

Following the solution procedure from [26], let us take the Laplace transform of (9). Taking into account that, initially, the system described by (9) is at thermal equilibrium and so $\frac{\partial\theta}{\partial\xi}|_{\xi=0} = 0$ and $\theta|_{\xi=0} = 0$, we have

$$\frac{d^2\Theta}{d\eta^2} - \left(2s + s^2\right)\Theta + \left[1 + \frac{1}{2}s\right]\tilde{Q} = 0, \tag{19}$$

where $\Theta(\eta; s)$ and $\tilde{Q}(\eta; s)$ are the Laplace transforms of $\theta(\eta, \xi)$ and $\tilde{q}(\eta, \xi)$, respectively. The general solution of the nonhomogeneous equation (19) is

$$Q(\eta; s) = C_1(s)e^{\lambda(s)\eta} + C_2(s)e^{-\lambda(s)\eta} + P(\eta; s), \tag{20}$$

where $\lambda(s) = \sqrt{2s + s^2}$. The two first terms on the right side of (20) are the general solution of the associated homogeneous equation with $\tilde{Q}(\eta; s) = 0$, and $P(\eta; s)$ is a particular solution of (19).

For the problem in question and taking into account the fact that the surface heat flux is induced by the electron gas after absorbing the laser energy, the boundary conditions become

$$\left.\frac{\partial\theta}{\partial\eta}\right|_{\eta=0} = -\tilde{q}'' - \frac{1}{2}\frac{\partial\tilde{q}''}{\partial\xi}, \qquad \lim_{\eta\to\infty}\theta = 0, \tag{21}$$

where $\tilde{q}'' = \frac{1}{\xi_p}\exp\left(-a[\frac{\xi-\xi_b}{\xi_p}]^2\right)$ is the dimensionless form of the surface heat flux. Hence, the parameter $C_1(s)$ must be zero, and (20) is simplified into

$$Q(\eta; s) = C(s)e^{-\lambda(s)\eta} + P(\eta; s). \tag{22}$$

To eliminate $C(s)$ from (22), the derivative of $\Theta(\eta; s)$ with respect to η is used:

$$\frac{dQ(\eta; s)}{d\eta} = -\lambda(s)C(s)e^{-\lambda(s)\eta} + \frac{dP(\eta; s)}{d\eta}. \tag{23}$$

Then, combining (22) and (23), and taking into account the relationship between the temperature gradient and the surface heat flux (21), the general solution of (20) can be written as

$$Q(\eta; s) = \frac{1 + \frac{1}{2}s}{\lambda(s)}\tilde{Q}''(s) + P(\eta; s) + \frac{1}{\lambda(s)}\frac{dP(\eta; s)}{d\eta}, \tag{24}$$

where $\tilde{Q}''(s)$ is the Laplace transform of $\tilde{q}''(s)$. The right part of (24) consists of the sum of two terms which are responsible for the temperature responses due to the surface heat flux and volumetric heating, respectively. Taking into account that the function $\tilde{Q}(\eta; s)$ can be represented as a

product of two functions, one of which depends on the complex variable s only, and the other is $\exp(-\eta/\Delta\eta)$, the particular solution of (20) can be written as follows:

$$P(\eta; s) = \Delta\eta^2 \frac{1 + \frac{1}{2}s}{\Delta\eta^2 s^2 + 2\Delta\eta^2 s - 1} \tilde{Q}(\eta; s). \quad (25)$$

References

1. D. Cahill, W. Ford, K. Goodson, G. Mahan, A. Majumdar, H. Maris, R. Merlin, S. Phillpot, J. Appl. Phys. **93**, 793 (2003)
2. A. Dietzel, R. Berger, P. Mächtle, M. Despont, W. Häberle, R. Stutz, G. Binnig, P. Vettiger, Sens. Actuators A, Phys. **100**, 123 (2002)
3. Y. Sun, D. Fangb, M. Sakaa, A.K. Soh, Int. J. Solids Struct. **45**, 1993 (2008)
4. S. Anisimov, B. Kapeliovich, T. Perel'man, Sov. Phys. JETP **39**, 375 (1974)
5. N. Singh, Int. J. Mod. Phys. B **24**, 1141 (2010)
6. D.Y. Tzou, *Macro to Microscale Heat Transfer: The Lagging Behavior* (Taylor & Francis, New York, 1997)
7. G. Eesley, Phys. Rev. B **33**, 2144 (1986)
8. W. Fann, R. Storz, H. Tom, J. Bokor, Phys. Rev. B **46**, 13592 (1992)
9. W. Fann, R. Storz, H. Tom, J. Bokor, Phys. Rev. Lett. **68**, 2834 (1992)
10. C. Sun, F. Vallee, L. Acioli, E. Ippen, J. Fujimoto, Phys. Rev. B **48**, 12365 (1993)
11. T.Q. Qiu, T. Juhasz, C. Suarez, W.E. Bron, C.L. Tien, Int. J. Heat Mass Transf. **37**, 2799 (1994)
12. R. Groeneveld, R. Sprik, A. Lagendijk, Phys. Rev. B **51**, 11433 (1995)
13. Z. Lin, L. Zhigilei, V. Celli, Phys. Rev. B **77**, 75133 (2008)
14. H. Sim, S. Park, T. Kim, Y. Choi, J. Lee, S. Lee, Mater. Trans. **51**, 1156 (2010)
15. T.Q. Qiu, C.L. Tien, Int. J. Heat Mass Transf. **37**, 2789 (1994)
16. J.J. Klossika, U. Gratzke, M. Vicanek, G. Simon, Phys. Rev. B **54**, 10277 (1996)
17. J. Chen, J. Beraun, Numer. Heat Transf., Part A, Appl. **40**, 1 (2001)
18. H. Inouye, K. Tanaka, I. Tanahashi, K. Hirao, Phys. Rev. B **57**, 11334 (1998)
19. H. Hirori, T. Tachizaki, O. Matsuda, O. Wright, Phys. Rev. B **68**, 113102 (2003)
20. D.W. Tang, N. Araki, J. Phys. D, Appl. Phys. **29**, 2527 (1996)
21. S. Link, C. Burda, M. Mohamed, B. Nikoobakht, M. El-Sayed, Phys. Rev. B **61**, 6086 (2000)
22. J. Shang, Z. Luo, C. Cong, J. Lin, T. Yu, G. Gurzadyan, Appl. Phys. Lett. **97**, 163103 (2010)
23. R. Rosei, D. Lynch, Phys. Rev. B **5**, 3883 (1972)
24. V.V. Kulish, L.J. Lage, J. Heat Transf. **122**, 372 (2000)
25. J.I. Frankel, J. Thermophys. Heat Transf. **20**, 945 (2006)
26. V.V. Kulish, L.J. Lage, L.P. Komarov, P.E. Raad, J. Heat Transf. **123**, 1133 (2001)
27. D. Joseph, L. Preziosi, Rev. Mod. Phys. **61**, 41 (1989)
28. M. Abramowitz, I. Stegun, *Handbook of Mathematical Functions with Formulas, Graphs, and Mathematical Tables* (US Government Printing Office, Washington, 2010)
29. V.V. Kulish, B.V. Novozhilov, Math. Probl. Eng. **4**, 173 (2003)
30. J. Hohlfeld, D. Grosenick, U. Conrad, E. Matthias, Appl. Phys. A Mater. **60**, 137 (1995). 129th WE-Heraeus-Seminar on Surface Studies by Nonlinear Laser Spectroscopies, Kassel, Germany, 30 May–1 June, 1994
31. J. Hohlfeld, J. Muller, S. Wellershoff, E. Matthias, Appl. Phys. B, Lasers Opt. **64**, 387 (1997)
32. W. Rohsenow, J. Hartnett, E. Ganic, *Handbook of Heat Transfer Fundamentals* (McGraw-Hill, New York, 1985)
33. G. Kaye, T. Laby, *Tables of Physical and Chemical Constants and Some Mathematical Functions* (Harlow, Longman, 1995)